Engineering 32 (2024) 163–173

Contents lists available at ScienceDirect

Engineering

journal homepage: www.elsevier.com/locate/eng

Research
Antimicrobial Resistance—Article

Dual Effects of Feed-Additive-Derived Chelerythrine in Combating Mobile Colistin Resistance

Huangwei Song [a,b,#], Xueyang Wang [a,b,#], Muchen Zhang [a,b], Zhiyu Zou [a,b], Siyuan Yang [a,b], Tian Yi [a,b], Jianfeng Wang [c], Dejun Liu [a,b], Yingbo Shen [a,b], Chongshan Dai [a,b], Zhihai Liu [d], Timothy R. Walsh [e], Jianzhong Shen [a,b], Congming Wu [a,b,*], Yang Wang [a,b,*]

[a] National Key Laboratory of Veterinary Public Health and Safety, College of Veterinary Medicine, China Agricultural University, Beijing 100193, China
[b] Guangdong Laboratory for Lingnan Modern Agriculture, Guangzhou 510642, China
[c] State Key Laboratory for Zoonotic Diseases, Key Laboratory of Zoonosis Research, Ministry of Education, Institute of Zoonosis, College of Veterinary Medicine, Jilin University, Changchun 130015, China
[d] College of Chemistry and Pharmaceutical Sciences, Qingdao Agricultural University, Qingdao 266109, China
[e] Ineos-Oxford Institute of Antimicrobial Research, Department of Biology, University of Oxford, Oxford OX1 3SZ, UK

ARTICLE INFO

Article history:
Received 3 November 2022
Revised 6 April 2023
Accepted 15 June 2023
Available online 6 September 2023

Keywords:
Chelerythrine
Antibiotic adjuvant
Conjugation inhibitor
Colistin
mcr-1
Dual effects

ABSTRACT

The emergence and spread of the mobile colistin-resistance gene, *mcr-1*, and its variants pose a challenge to the use of colistin, a last-resort antibiotic used to treat severe infections caused by extensively drug-resistant (XDR) Gram-negative pathogens. Antibiotic adjuvants are a promising strategy to enhance the efficacy of colistin against colistin-resistant pathogens; however, few studies have considered the effects of adjuvants on limiting resistance-gene transmission. We found that chelerythrine (4 mg·L^{-1}) derived from *Macleaya cordata* extract, which is used as an animal feed additive, reduced the minimal inhibitory concentration (MIC) of colistin against an *mcr-1* positive *Escherichia coli (E. coli)* strain by 16-fold (from 2.000 to 0.125 mg·L^{-1}), eliminated approximately 10^4 colony-forming units (CFUs) of an *mcr-1*-carrying strain in a murine intestinal infection model, and inhibited the conjugation of an *mcr-1*-bearing plasmid *in vitro* (by > 100-fold) and in a mouse model (by up to 5-fold). A detailed analysis revealed that chelerythrine binds to phospholipids on bacterial membranes and increases cytoplasmic membrane fluidity, thereby impairing respiration, disrupting proton motive force (PMF), generating reactive oxygen species (ROS), and decreasing intracellular adenosine triphosphate (ATP) levels, which subsequently downregulates *mcr-1* and conjugation-associated genes. These dual effects of chelerythrine can expand the use of antibiotic adjuvants and may provide a new strategy for circumventing mobile colistin resistance.

1. Introduction

Antimicrobial agents have prolonged human life, promoted food production, and positively affected global public health. Colistin, a non-ribosomal peptide antibiotic, is among the few last-resort antibiotics for treating carbapenem-resistant *Enterobacteriaceae*; it has been used as a critically important veterinary drug in food-producing animals for over 60 years [1,2]. However, the widespread and extensive use of colistin in healthcare settings and agriculture was found to accelerate the emergence of mobile colistin-resistance gene, *mcr-1*, in 2016 and its variants soon after [3,4]. The MCR-1 enzyme decreases the negative charge of bacterial lipopolysaccharides by adding phosphoethanolamine to lipid A, thereby reducing colistin's affinity for the bacterium and causing resistance [3,5,6]. Notably, colistin promotes the horizontal gene transfer of *mcr-1* via various plasmids [7], thus assisting *mcr-1* in further spreading globally across six continents [4]. The transmission of *mcr* variants and the bacterial pathogens that carry them in animals, foods, and the environment will inevitably and eventually harm humans [8,9], and the high *mcr-1* carriage in the human gut poses a substantial risk to colistin use in clinical practice [10]. Therefore, strategies are urgently needed to overcome *mcr-1*-mediated colistin-resistant pathogens.

* Corresponding authors.
E-mail addresses: wucm@cau.edu.cn (C. Wu), wangyang@cau.edu.cn (Y. Wang).
# These authors contributed equally to this work.

https://doi.org/10.1016/j.eng.2023.06.012

Antimicrobial chemotherapy remains the main strategy for combating bacterial infections. However, traditional antimicrobial development has become increasingly time-consuming and expensive [11,12]. Most antibiotic scaffolds in clinical use today were discovered in 1950–1980 [13]. More worryingly, an increasing gap exists between the emergence and spread of novel antimicrobial resistance genes and new antimicrobial development, which is one of the main factors leading to the antimicrobial resistance crisis. Combining antimicrobial agents with synergistic effects is a potential approach to combat this problem [14,15]. However, combining traditional antimicrobial agents may be ineffective, due to the wide dissemination of extensively drug-resistant (XDR) pathogens that exhibit resistance to most classes of commonly used antimicrobial agents. Inspired by the concept and success of antibiotic adjuvants [16,17], exploring compounds with novel targets is a promising strategy to enhance the activity of existing antimicrobial agents.

Natural compounds are considered a major resource for novel antibiotics or antibiotic adjuvants [18,19]. For example, prenylated flavonoids and pterostilbene, which respectively target the bacterial membrane and the MCR-1 enzyme, restore colistin activity against *mcr-1*-positive *Escherichia coli* (*E. coli*) strains [20,21]. However, plasmid-mediated *mcr-1* can constantly and easily transfer among bacterial pathogens in patients during antibiotic chemotherapy, making the therapy more difficult [22]. Thus, ideal adjuvants should act synergistically with antibiotics against XDR bacteria and inhibit XDR gene transfer. Screening natural compounds with such dual effects may therefore help combat the antimicrobial resistance crisis. Herein, we identify and evaluate chelerythrine (CHE), a dual-effect natural compound and a major active ingredient of *Macleaya cordata* extract (Sangrovit), which is used worldwide in feed additives to promote animal growth.

2. Materials and methods

2.1. Materials and bacterial strains

A natural compound library was purchased from TargetMol (Cat No. L6000, purity > 95%; USA). The *mcr-1* bearing plasmid IncI2-*mcr-1* was extracted from ZJ807 and then transformed into *E. coli* BW25113 to form BW25113::IncI2-*mcr-1*, which was applied in screening and conjugation assays as the donor bacterium, while *E.coli* J53 with sodium azide resistance was applied as the recipient bacterium. The lab-preserved wild *mcr-1*-positive *E. coli* strain ZJ807 was applied in antimicrobial susceptibility tests and mechanism exploration experiments [10].

2.2. Cell-based antimicrobial combination screening

Approximately 2592 natural compounds isolated from plant, animal, and microbial sources were screened against *E. coli* BW25113::IncI2-*mcr-1* in combination with 0.5 μg·mL^{-1} (1/4× minimum inhibitory concentration (MIC)) colistin. The screening protocol was performed according to the Clinical & Laboratory Standards Institute (CLSI) guidelines (M45-A2). Further details are provided in Appendix A.

2.3. Fractional inhibitory concentration (FIC) index determination

FIC indices were measured via checkerboard assay according to the CLSI guidelines (M45-A2). Each compound was serially diluted 2-fold in cation-adjusted Mueller-Hinton broth (CAMHB) to create an 8 × 8 matrix with a final volume of 100 μL. Overnight-grown *mcr*-positive or -negative strains were diluted 1:100 into fresh Mueller-Hinton broth (MHB) and incubated at 37 °C for 4–6 h. The log phase culture was adjusted to match a 0.5 McFarland turbidity standard, followed by 1:100 dilution in CAMHB. Then, 100 μL of diluted bacterial suspension was added to each well of the 8 × 8 matrix and incubated at 37 °C for 18 h. The optical density at 600 nm (OD_{600}) was measured using an Infinite M200 Microplate reader (Tecan, Switzerland). At least two replications were done for each combination, and the means were used for calculations. The FIC calculation was performed according to the following formula:

$$\text{FIC index} = MIC_{ab}/MIC_a + MIC_{ba}/MIC_b = FIC_a + FIC_b$$

where $MIC_{a/b}$ is the MIC of compound A/B alone, MIC_{ab} is the MIC of compound A in combination with compound B, MIC_{ba} is the MIC of compound B in combination with compound A, and $FIC_{a/b}$ is the FIC of compound A/B. Synergy is defined as an FIC index of ≤ 0.5.

2.4. Adenosine triphosphate (ATP) determination

The intracellular ATP level of *E. coli* ZJ807 was determined using an Enhanced ATP Assay Kit (Cat No. S0027; Beyotime, China). ZJ807 grown overnight was diluted 1:100 in fresh Luria-Bertani (LB) broth and incubated at 37 °C for 4–6 h. Then, the culture was collected via centrifuging (4000 r·min^{-1}) and resuspended in 0.1 mol·L^{-1} of phosphate-buffered saline (PBS; pH 7.4) to obtain an OD_{600} of 0.5. After treatment with varying concentrations (0, 1×, 2×, or 4× MIC) of CHE for 30 min, the bacterial cultures were collected via centrifuge (12 000 r·min^{-1}, 5 min, 4 °C). The precipitates were lysed by lysozyme resolved in Tris-ethylene diamine tetraacetic acid (EDTA-TE) buffer (1 mg·mL^{-1}) and recentrifuged, and the supernatants were used to determine the intracellular ATP level. Detecting solution was added to a 96-well plate and incubated for 5 min at room temperature. Then, the supernatants were added to the well and mixed quickly, and the luminescence was measured with an Infinite M200 microplate reader. In conjugation assays with different CHE concentrations (2, 4, or 8 μg·mL^{-1}), the intracellular ATP levels of the donor and recipient bacteria were determined using the above method.

2.5. Iodonitrotetrazolium chloride (INT) reduction assay

The overnight-grown *E. coli* strain ZJ807 was diluted 1:100 in fresh LB broth and incubated at 37 °C for 4–6 h to reach the exponential phase. After being washed and resuspended in PBS (pH 7.4, 0.1 mol·L^{-1}) to reach an OD_{600} of 0.3, the cell suspension was kept on ice. In glass tubes, CHE (0, 1/2×,1×, or 2× MIC) was added in buffer with 1 mmol·L^{-1} iodonitrotetrazolium chloride (INT) and cell suspension. The tubes were mixed vigorously and incubated at 30 °C. The absorbance at 490 nm was read at 10 min intervals.

2.6. Proton motive force (PMF) measurement assay

The PMF is composed of the pH gradient (ΔpH) and the membrane potential ($\Delta\Psi$). The effects of CHE on the $\Delta\Psi$ of *E. coli* ZJ807 were determined using the membrane potential-sensitive cyanine dye, $DiSC_3(5)$ (Cat No. D131315; Aladdin, China). The ΔpH changes of ZJ807 after treatment with CHE (0, 1/2×, 1×, or 4× MIC) were determined using another pH-sensitive fluorescence probe, BCECF-AM (Cat No. S1006; Beyotime, details provided in Appendix A).

2.7. Membrane fluidity assay

The membrane fluidity of *E. coli* ZJ807 was determined by means of Laurdan generalized polarization (GP), as previously described [23], with some modifications. First, the spheroplasts of ZJ807 were prepared as previously described [24]. In brief,

overnight cultures of ZJ807 were washed twice, resuspended in CAMHB, and then added at a final inoculum of 10^8 colony-forming units (CFUs)·mL^{-1} to 9 mL of CAMHB. After incubation for 2 h, the strain was washed twice by centrifuging (4 °C, 20 min, 3273*g*). Next, it was resuspended, first in 10 mL of Tris buffer (0.03 mol·L^{-1}, pH 8.0), and then in Tris buffer containing 20% sucrose (pH 8.0, 0.03 mol·L^{-1}). Subsequently, 1 mL of lysozyme (10 mg·mL^{-1}) and 250 μL of EDTA (10 mg·mL^{-1}) were added to remove the cell wall and outer membrane, respectively. The suspension was incubated for 1 h at 30 °C. Then, 500 μL of trypsin (10 mg·mL^{-1}) was added, and the suspension was further incubated for 15 min at 30 °C. The spheroplasts were harvested via centrifugation 4 °C, 20 min, 2000*g*. The spheroplasts of ZJ807 were then stained with Laurdan, with a final concentration of 10 μmol·L^{-1}, for 10 min at room temperature in the dark, under agitation. Subsequently, the cells were treated with 1/2×, 1×, or 2× MIC concentrations of CHE or benzyl alcohol (10 mmol·L^{-1}) for 35 min. Finally, Laurdan fluorescence was measured at 435 and 490 nm following excitation at 350 nm. The Laurdan GP was calculated using the following formula:

$$GP = (I435 - I490)/(I435 + I490)$$

where I435 and I490 denotes the fluorescence intensity of the Laurdan fluorescent probe at a wavelength of 435 and 490 nm, respectively. All experiments were performed with at least three biological replicates.

2.8. Antimicrobial activity of mixtures of CHE and lipids

To evaluate the effect of different lipids on the antimicrobial activity of CHE, CHE (1000 μg·mL^{-1}) was mixed with 25 mmol equivalents of lipopolysaccharide (LPS), phosphatidylethanolamine (PE), phosphatidylglycerol (PG), or cardiolipin (CL). The mixtures were incubated at 37 °C for 30 min and then added to blank diffusion discs. Once dried, the discs were placed on a Mueller-Hinton agar (MHA) plate containing *E. coli* 25922. After overnight culture at 37 °C, the inhibition zones of the mixtures were measured.

2.9. Transcription level of mcr-1 via reverse transcription-polymerase chain reaction (RT-PCR)

The total RNA was extracted using the EASYspin Plus kit (Cat No. RN0801; Aidlab, China). 1 μg of RNA was reverse transcripted using the PrimeScript RT reagent kit (Cat No. RR047A; Takara, Japan). The messenger RNA (mRNA) levels of *mcr-1* relative to the control genes (16S ribosomal RNA49) were determined by means of quantitative RT-PCR (qRT-PCR) with a SYBR Premix Ex Taq qPCR kit (Cat No. RR820A; Takara). RT-PCR was performed using an ABI QuantStudio 7 detection system (Applied Biosystems, USA). The fold changes in the gene expression were determined using the $2^{-\Delta\Delta Ct}$ method.

2.10. MCR-1 expression assay

Overnight-grown *E. coli* strain BL21(DE3)::pET28a-*mcr-1* with a 6× His tag at the N terminus from the previous study was diluted 1:100 with fresh LB broth and cultured at 37 °C for 4 h. Next, the cells were treated with different final concentrations of CHE (0, 16, 32, or 64 μg·mL^{-1}) and 0.4 mmol·L^{-1} isopropyl-β-*D*-thiogalacto-pyranoside (IPTG) and cultured for another 4 h. After being collected via centrifuging, the cells were boiled with the 6× loading buffer, and 10 μg of each sample was subjected to sodium dodecyl-sulfate polyacrylamide gel electrophoresis (SDS-PAGE) and transferred to a polyvinylidene difluoride membrane, which was further sealed and coated with antibodies (His-tag rabbit mAb, Cat No. 12698; Cell Signaling Technology, USA; mouse monoclonal [GA1R] to GAPDH, Cat No. ab125247; Abcam, UK; HRP-labeled goat anti-rabbit IgG(H+L), Cat No. A0208; Beyotime; HRP-labeled goat anti-mouse IgG(H+L), Cat No. A0216; Beyotime). The blots were then observed using a Western blotting visualizer (Tanon-5200; Bio-Tanon, UK).

2.11. Conjugation inhibition assay

The donor (*E. coli* BW25113-carrying IncI2 plasmid) with resistance genes of colistin (*mcr-1*) and the recipient bacteria (*E. coli* J53) were cultured in brain–heart infusion (BHI) broth with the corresponding antibiotics overnight at 37 °C and 200 r·min^{-1} for 16 h. The overnight cultures were diluted ten times into 2 mL of BHI drug-free broth at 37 °C for 4 h. Then, the OD_{600} of the donor and recipient bacteria was adjusted to be consistent (~10^8–10^9-CFUs·mL^{-1}). Next, the donor and recipient bacteria were mixed in a 1:1 ratio and centrifuged at 4000 r·min^{-1} for 5 min, and the precipitate was collected and suspended in 2 mL of BHI broth with different concentrations of compounds for 16 h, with a drug-free BHI broth group as a control. After incubation at 37 °C for 16 h without shaking, 100 μL of each of the mixtures was spread onto BHI agar plates containing sodium azide and colistin at a suitable concentration for 24 h. The numbers of transconjugants and recipients were then respectively counted. The conjugative transfer frequency was calculated by dividing the number of transconjugants detected by the total number of recipients. All conjugation experiments were conducted with at least three biological replicates. Meanwhile, donor and recipient bacteria were plated on double resistant plates to exclude spontaneous mutation.

2.12. Mouse gut infection model

To disrupt colonization resistance and enable infection with *E. coli* ZJ807, all mice (n = 28) were intragastrically administered ampicillin (1.0 mg·mL^{-1}), vancomycin (0.5 mg·mL^{-1}), clindamycin (0.5 mg·mL^{-1}), and metronidazole (1.0 mg·mL^{-1}) every 24 h for 72 h. Antibiotic-treated mice were given 24 h to recover, prior to infection with ZJ807. A total of 6×10^7 CFUs of ZJ807 was delivered via oral gavage, and mice were randomly assigned to seven treatment groups, each group containing four mice. After 4 h of ZJ807 challenge, mice were orally gavaged with PBS, colistin (2 and 4 mg·kg^{-1}) or CHE (64 and 128 mg·kg^{-1}) alone, or a combination of colistin with CHE ((2 + 64) mg·kg^{-1} and (4 + 128) mg·kg^{-1}). To monitor ZJ807 loads in the gut, fecal samples were collected, weighed, homogenized, serially diluted, and quantified using China Blue agar (CBA, Cat No. CM903; Landbridge, China) plates supplemented with 2 μg·mL^{-1} colistin.

2.13. In vivo conjugation assay in mice

Mice were pretreated with four antibiotics, including ampicillin (1.0 mg·mL^{-1}), vancomycin (0.5 mg·mL^{-1}), clindamycin (0.5 mg·mL^{-1}), and metronidazole (1.0 mg·mL^{-1}), for three days to remove colonization resistance. Then, six mice were each treated orogastrically with approximately 10^8 CFUs of *E. coli* J53 and, 24 h later, with about 10^8 CFUs of ZJ807. After the intragastric administration of donor and recipient bacteria, 10 mg·kg^{-1} CHE and PBS as the control were gavaged into the intestinal tract of the mice every day. Feces were collected daily in 1 mL of PBS with glass beads for vortex mixing. Bacteria populations were measured via selective plating on China Blue media (selection for donor and transconjugants was done with colistin (2 μg·mL^{-1}); that for recipients and transconjugants was done with NaN_3 (150 μg·mL^{-1}); and that for transconjugants was done with colistin and NaN_3), and the final conjugative transfer frequency was calculated by dividing the

number of transconjugants detected by the total number of recipients.

2.14. Statistical analyses

GraphPad Prism 9 was used for data processing. All data were presented as the mean ± standard deviation (s.d.) For the *in vitro* studies, a one-way analysis of variance (ANOVA) with Dunnett's multiple comparisons was used to calculate *P* values. For the *in vivo* studies, *n* represents the number of animals per group, and the statistical significance was determined by means of a Mann–Whitney *U* test. Differences with $P < 0.05$ were considered significant.

3. Results

3.1. CHE is a potent colistin adjuvant both in vitro and in vivo

To identify natural compounds that can potentiate colistin activity, we isolated and screened 2592 natural compounds from plants, animals, and microbial sources by combining them with 1/4× MIC of colistin. We then assessed their ability to inhibit the growth of the *mcr-1*-positive *E. coli* strain BW25113::IncI2-*mcr-1* (Fig. 1(a)). Using 90% growth inhibition as the cutoff, we identified 120 molecules—mainly flavonoids and alkaloids (Fig. S1(a) in Appendix A)—that were synergistic with colistin and showed bacterial growth-inhibiting activity (Fig. 1(b)). Because flavonoids

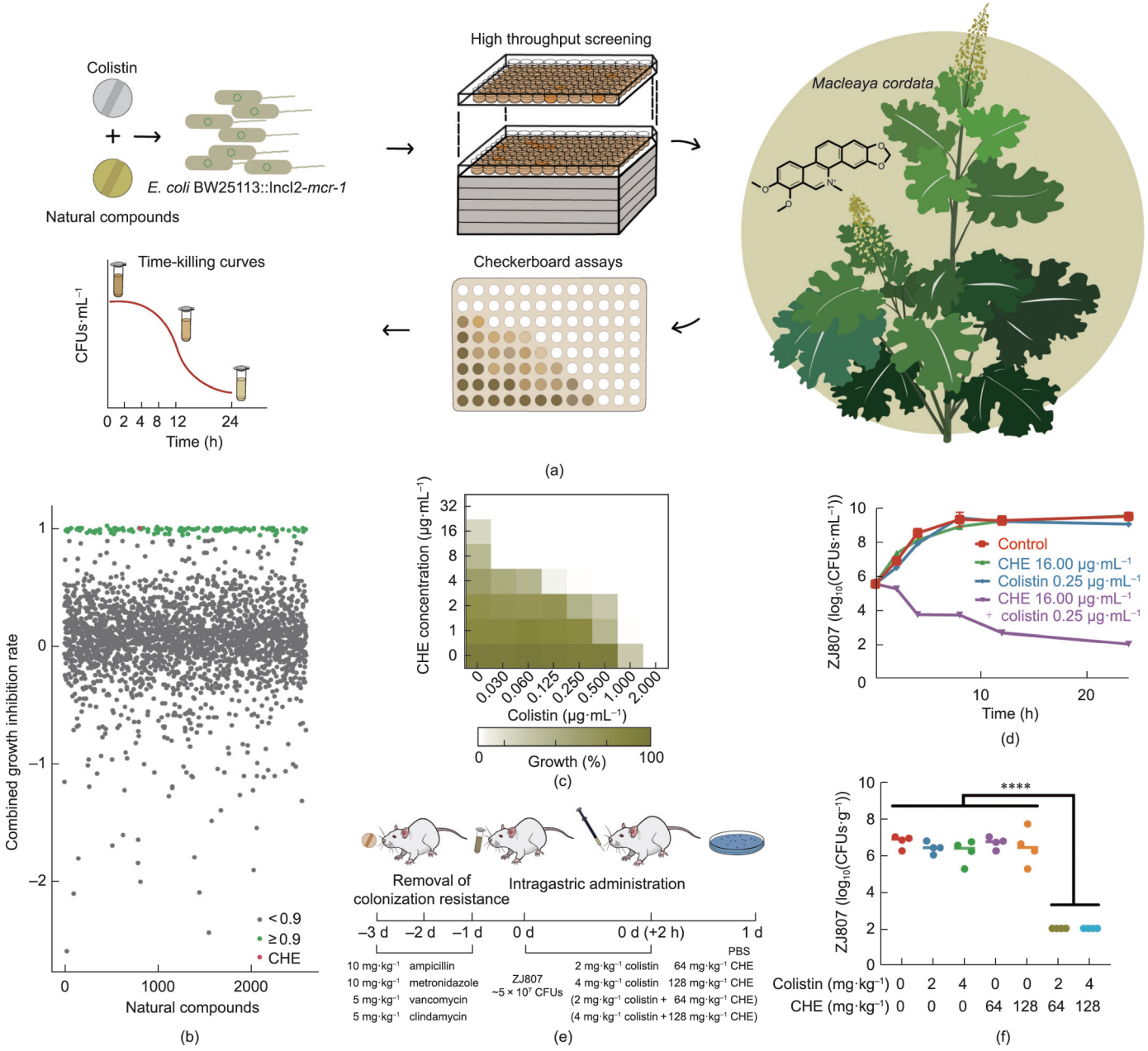

Fig. 1. Screening of colistin adjuvants and the synergistic effect between CHE and colistin *in vitro* and *in vivo*. (a) Scheme for screening colistin adjuvants. (b) Primary screening data for the growth inhibition of BW25113::IncI2-*mcr-1* by 1/4× MIC of colistin plus 50 μmol·L^{-1} of 2592 molecules within the natural compounds library. Shown is the mean of two biological replicates. Green are growth inhibitory molecules; gray are non-growth inhibitory molecules. (c) Growth inhibition checkerboards of CHE with colistin against *E. coli* ZJ807. Synergy is defined as a FIC index ≤ 0.5. (d) Time-killing curves of ZJ807 for treatment with CHE or colistin alone, and the combination of CHE and colistin. (e) Experimental design for the mouse intestinal infection model and treatment. (f) Bacterial load of ZJ807 in the feces of infected mice with different treatment. The *P* value in part (f) was determined using a two-sided, Mann–Whitney *U* test. ****$P < 0.0001$.

have previously been shown to enhance colistin efficacy against Gram-negative pathogens [20], we focused on alkaloids and found that CHE exhibited a synergistic effect with colistin against the *mcr-1*-carrying *E. coli* strain ZJ807 (FIC index = 0.25), *mcr-8*-positive *Klebsiella pneumoniae* (*K.pneumoniae*) KP91 (FIC index ≤ 0.25), and *mcr-9*-positive *Salmonella Typhimurium* (*S. Typhimurium*) ST5 (FIC index ≤ 0.125), indicating that CHE is a non-specific inhibitor of MCR-1 (Fig. 1(c); Figs. S1(b) and (c) in Appendix A). In addition, the combination of CHE and colistin showed a synergistic effect on the *mcr*-negative *E. coli* strain BW25113 (FIC index = 0.5; Fig. S1(d) in the Appendix A), implying that the potentiating effect of CHE on colistin was partly due to *mcr*. Furthermore, the combination of CHE and colistin yielded a nearly 4-$\log_{10}$ reduction in the CFUs of ZJ807 after 24 h, whereas neither CHE nor colistin alone exhibited an obvious killing effect (Fig. 1(d)). To evaluate this synergistic effect *in vivo*, we intragastrically administered ZJ807 (1.0×10^7 CFUs) to a mouse intestinal infection model (Fig. 1(e)). This combination significantly cleared ZJ807 from the mouse model fecal samples (100 CFUs, under the test line), whereas the ZJ807 loads in the mice treated with either CHE or colistin alone resembled those of the control group (1.0×10^6 to 1.0×10^7 CFUs; Fig. 1(f) in Appendix A).

3.2. CHE exerted antibacterial effects by interfering with bacterial energy metabolism

To understand the synergistic effect of CHE and colistin, we first explored the antimicrobial mechanism of CHE. ZJ807 cells treated with CHE exhibited a dose-dependent reduction in both intracellular and extracellular ATP levels (Fig. 2(a); Fig. S2(a) in the Appendix A), suggesting that the ATP decrease was not due to membrane damage. To further confirm this suggestion, we used the fluorescence probe propidium iodide to determine the membrane permeability and observed that CHE bound itself to propidium iodide and quenched the fluorescence (Fig. S2(b) in the Appendix A). In the supernatants of bacterial cultures after treatment with different CHE doses, we found no significant activity changes in β-galactosidase, which is cryptic outside of bacteria unless there is damage to the membrane permeability; this confirmed that the bactericidal effect of CHE was not due to damage to membrane permeability (Fig. S2(c) in the Appendix A). Since the generation of ATP is mainly driven by the PMF, which comprises ΔpH and $\Delta\Psi$, we found that ΔpH was dose-dependently dissipated in CHE-treated ZJ807 (Fig. 2(b)), while the $\Delta\Psi$ was significantly increased in ZJ807 after CHE treatment, to attempt to maintain a

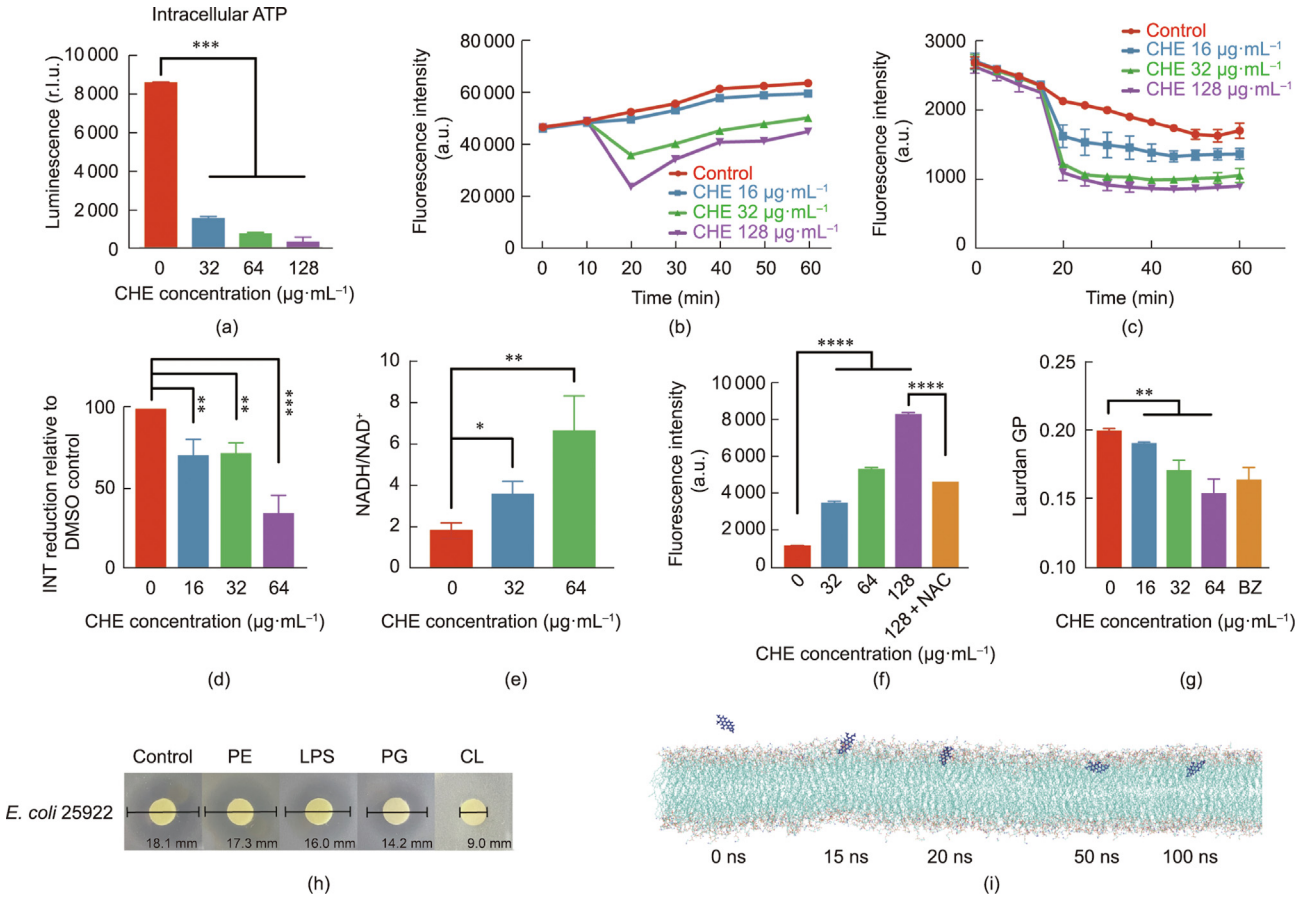

Fig. 2. Antimicrobial mechanism of CHE. (a) Decreased levels of intracellular ATP in *E. coli* ZJ807 after treatment with CHE. Changes in (b) ΔpH and (c) $\Delta\Psi$ of ZJ807 treated with CHE. (d) Cellular respiratory level of ZJ807 treated with CHE. (e) Increase in ratios of NADH to NAD^+ from treatment with different dosages of CHE. (f) ROS levels of ZJ807 after challenged with different concentrations of CHE. (g) Changes in plasma membrane fluidity of ZJ807 after treatment with CHE; 10 mmol·L^{-1} benzyl alcohol (BZ) was used as the positive control. (h) Exogenous addition of PG and CL abolishes the antibacterial activity of CHE against *E. coli* 25922. Inhibition zones of the mixtures of CHE (1000 μg·mL^{-1}) and 25 mmol·L^{-1} of PE, LPS, PG, and CL against *E. coli* 25922 for overnight incubation at 37 °C. (i) Molecular dynamics simulations of CHE binding to 75%:25%:5% PE/PG/CL bilayers (100 ns). a.u.: arbitrary units; r.l.u.: relative light unit. *P* value was detected using one-way ANOVA and corrected using the Dunnett method. $^*P < 0.05$, $^{**}P < 0.01$, $^{***}P < 0.001$, $^{****}P < 0.0001$.

steadier PMF as the ΔpH decreased (Fig. 2(c)). Furthermore, CHE and kanamycin worked synergistically in ZJ807 (FIC index = 0.3125), and the intracellular accumulation of kanamycin depended on $\Delta\Psi$. However, CHE and doxycycline were not synergistic (FIC index = 3), as the intracellular transport of doxycycline relied on the ΔpH (Fig. S2(d) in Appendix A), confirming the PMF disruption in ZJ807 after CHE treatment.

Given that ΔpH is generated by the electron transport chain (ETC), we measured the activity of the ETC in ZJ807 by testing its ability to reduce int (an activity indicator of the ETC), which can be reduced to a red insoluble formazan by components of the prokaryotic respiratory chain [25]. CHE (16–64 μg·mL^{-1}) decreased the reduction of INT to red insoluble formazan by approximately 50% compared with the untreated controls (Fig. 2(d)), which suggested an impaired electron transport process in the ETC and was consistent with the disrupted PMF. Moreover, the NADH/NAD$^+$ ratio in CHE-treated cells increased by up to 3-fold (P = 0.0087, Fig. 2(e)), further confirming that CHE depleted the bacterial ATP by decreasing ETC activity [26]. Similar to a previous report [27], high NADH/NAD$^+$ ratios were accompanied by CHE dose-dependent reactive oxygen species (ROS) generation (Fig. 2(f)). Notably, the ROS scavenger *N*-acetylcysteine (NAC) (6 mmol·L^{-1}) partially recovered bacterial intracellular ATP levels (Fig. S2(e) in Appendix A), indicating that ROS is one factor in ATP depletion. Moreover, another ROS scavenger, thiourea, partly impaired the killing ability of CHE (Fig. S2(f) in Appendix A), indicating that ROS are involved in the antimicrobial mechanisms of CHE. Therefore, CHE decreased the cellular respiration, disrupted the PMF, and generated ROS, thereby depleting intercellular ATP. However, the mechanism of CHE-mediated impaired cellular respiration required further investigation.

3.3. CHE targeted the bacterial inner membrane and increased its fluidity

Changes in plasma membrane fluidity can impair cellular respiration, largely due to the delocalization of respiratory chain complexes [23,28]. Application of the fluorescence polarization probe Laurdan [29] revealed that the membrane fluidity of CHE-treated *E. coli* ZJ807 was significantly increased (Fig. 2(g)). We therefore hypothesized that CHE might interact with phospholipids in the plasma membrane to increase membrane fluidity. As expected, the exogenous addition of bacterial phospholipids (PG and CL) dose-dependently diminished CHE activity (Fig. 2(h)). We performed molecular dynamics simulations to further explore the interaction mechanisms of CHE and phospholipids [23,30]. CHE was initially recruited to the membrane surface by binding the methylenedioxy group to the hydrophilic lipid heads. After approximately 10 ns of sustained attachment, CHE began to penetrate the membrane interior perpendicularly or obliquely to the cell membrane surface, maximizing the interactions between the nonpolar benzene rings and hydrophobic lipid tails. After 45 ns, CHE was completely embedded in the outer leaflet of the lipid bilayer (Fig. 2(i)). These simulations demonstrated that the methylenedioxy groups and hydrophobicity of the CHE core rings play important roles in membrane attachment and penetration.

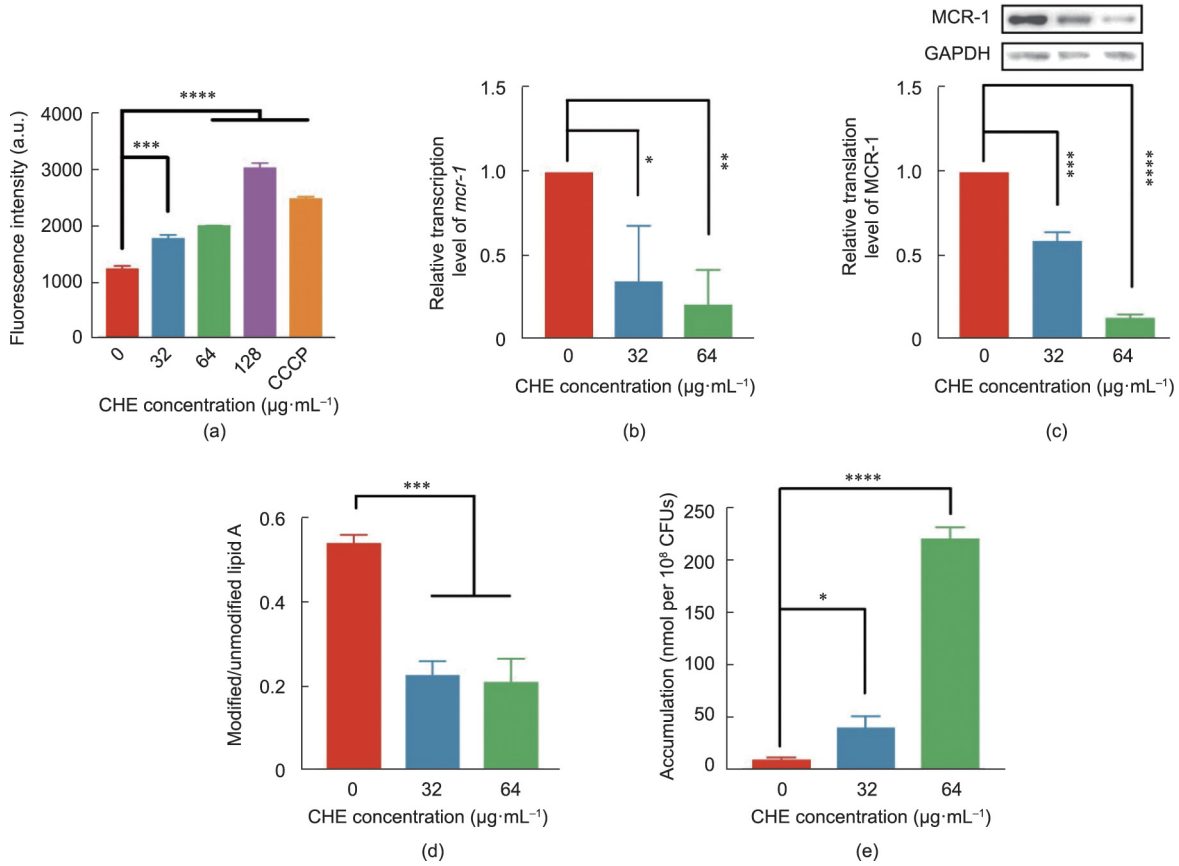

Fig. 3. Synergistic mechanism of CHE to potentiate colistin. (a) Activity of efflux pumps of ZJ807 treated with different concentrations of CHE; 10 μg·mL^{-1} of CCCP served as the positive control. (b) Decrease in the relative transcription level of *mcr-1* in ZJ807 treated with CHE. (c) Decrease in the relative translation level of *mcr-1* in *E. coli* strain BL21(DE3)::pET28a-*mcr-1* treated with CHE. GAPDH is the loading control. (d) Changes in the ratios of modified to unmodified lipid A of ZJ807 treated with CHE. (e) Accumulations of colistin in ZJ807 treated with CHE. *P* value was detected using one-way ANOVA and corrected using the Dunnett method. *P < 0.05, **P < 0.01, ***P < 0.001, ****P < 0.0001.

3.4. CHE potentiated colistin efficacy by limiting the function of efflux pumps and mcr-1

Since the bacterial efflux pumps and *mcr-1* and its variants are colistin resistance factors [3,31,32], and because CHE significantly disrupted the PMF and reduced intracellular ATP levels, we hypothesized that CHE might potentiate the efficacy of colistin by weakening the function of the efflux pumps and *mcr-1*. We found that the efflux activity was dose-dependently impaired by CHE (Fig. 3(a)). With 128 μg·mL^{-1} of CHE, the intracellular ethidium bromide (EB) fluorescence was 2-fold higher than that of the control group ($P < 0.0001$). Furthermore, *mcr-1* transcription levels in CHE-treated ZJ807 were up to 4-fold lower ($P = 0.003$; Fig. 3(b)), and MCR-1 expression levels in CHE-treated *E. coli* BL21(DE3)::pET28a-*mcr-1* were dose-dependently decreased by up to 10-fold ($P < 0.0001$; Fig. 3(c)). Moreover, applying CHE decreased the ratio of modified/unmodified lipid A in ZJ807 by > 50% ($P = 0.0008$; Fig. 3(d)). In addition, CHE treatment increased the intercellular concentrations of colistin in ZJ807 by > 15-fold ($P < 0.0001$; Fig. 3(e)), indicating that CHE restored colistin activity against *mcr-1*-positive strains by reducing lipid A modification and increasing intercellular drug concentrations by diminishing the intracellular ATP levels.

3.5. CHE inhibited conjugation of the IncI2 plasmid carrying mcr-1 in vitro and in vivo

As decreasing intracellular ATP levels can undermine the conjugation process, we explored whether CHE affects *mcr-1* conjugation. CHE at 2, 4, and 8 μg·mL^{-1} had no significant bactericidal effects on the growth curves of either the donor or recipient (Fig. 4(a)); thus, we monitored the conjugation frequency rates of the *mcr-1*-bearing IncI2 plasmid under 0, 2, 4, or 8 μg·mL^{-1} of CHE. Compared with the natural spontaneous conjugation frequency (1.99×10^{-1}), CHE significantly and dose-dependently decreased the conjugation frequencies of IncI2 (8.46×10^{-2} to 1.55×10^{-3}), with a > 125-fold decrease at 8 μg·mL^{-1} of CHE ($P = 0.0002$; Fig. 4(b)). We further used mice to verify the *in vivo* effect of CHE on *mcr-1* conjugation (Fig. 4(c)). The conjugation efficiency of the IncI2 *mcr-1*-carrying plasmid in the mouse intestines was similar to that *in vitro* (10^{-3} to 10^{-1}), and the average transfer frequency in the CHE-treated group (1.87×10^{-3}) on day 1 was five times lower than that in the control group (1.02×10^{-2}; $P = 0.002$; Fig. 4(d)). Although the decrease in both recipient bacteria and transconjugants in the mouse intestines on subsequent days may have led to a gradually increased transfer frequency, the inhibition of the conjugative transfer frequency in the CHE-treated group as a whole was approximately twice as effective as that in the control group (Fig. 4(d)).

3.6. CHE limited the energy source for conjugative transfer and suppressed the expression of conjugation-related genes

Conjugative transfer among bacteria is an energy-consuming process, involving DNA replication and type IV secretion system (T4SS) assembly [33]. Although high CHE concentrations (32–128 μg·mL^{-1}) can decrease bacterial ATP levels, it remains unclear whether low concentrations (2–8 μg·mL^{-1}) decrease bacterial ATP levels and subsequently inhibit conjugation rates. Compared with those of the control group, 2–8 μg·mL^{-1} CHE significantly decreased the intracellular ATP contents of the donor (73%–88%) and recipient (52%–76%) bacteria ($P < 0.05$; Fig. 5(a)). Moreover, the transcriptome data showed an approximately 2-fold

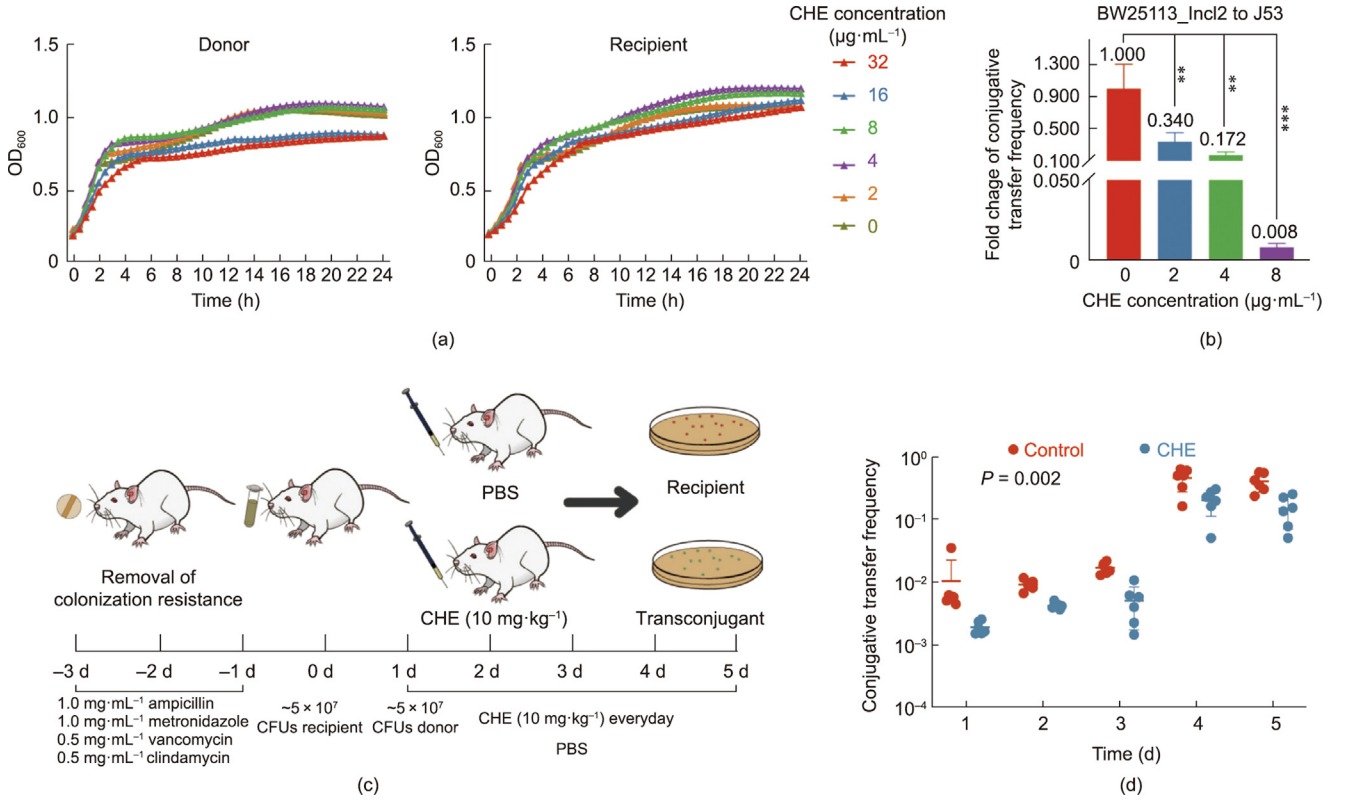

Fig. 4. Effects of CHE on the conjugative transfer of plasmid IncI2 *in vitro* and *in vivo*. (a) Growth curve of donor and recipient bacteria under different CHE concentrations. (b) Fold change in the conjugative transfer frequency *in vitro*. (c) Scheme of the experimental protocols for conjugative transfer *in vivo*. (d) Conjugative transfer frequency *in vivo* ($n = 6$). *P* value was detected using one-way ANOVA and corrected using the Dunnett method. $^{**}P < 0.01$, $^{***}P < 0.001$. Another *P* value in part (d) was determined using a two-sided, Mann–Whitney *U* test.

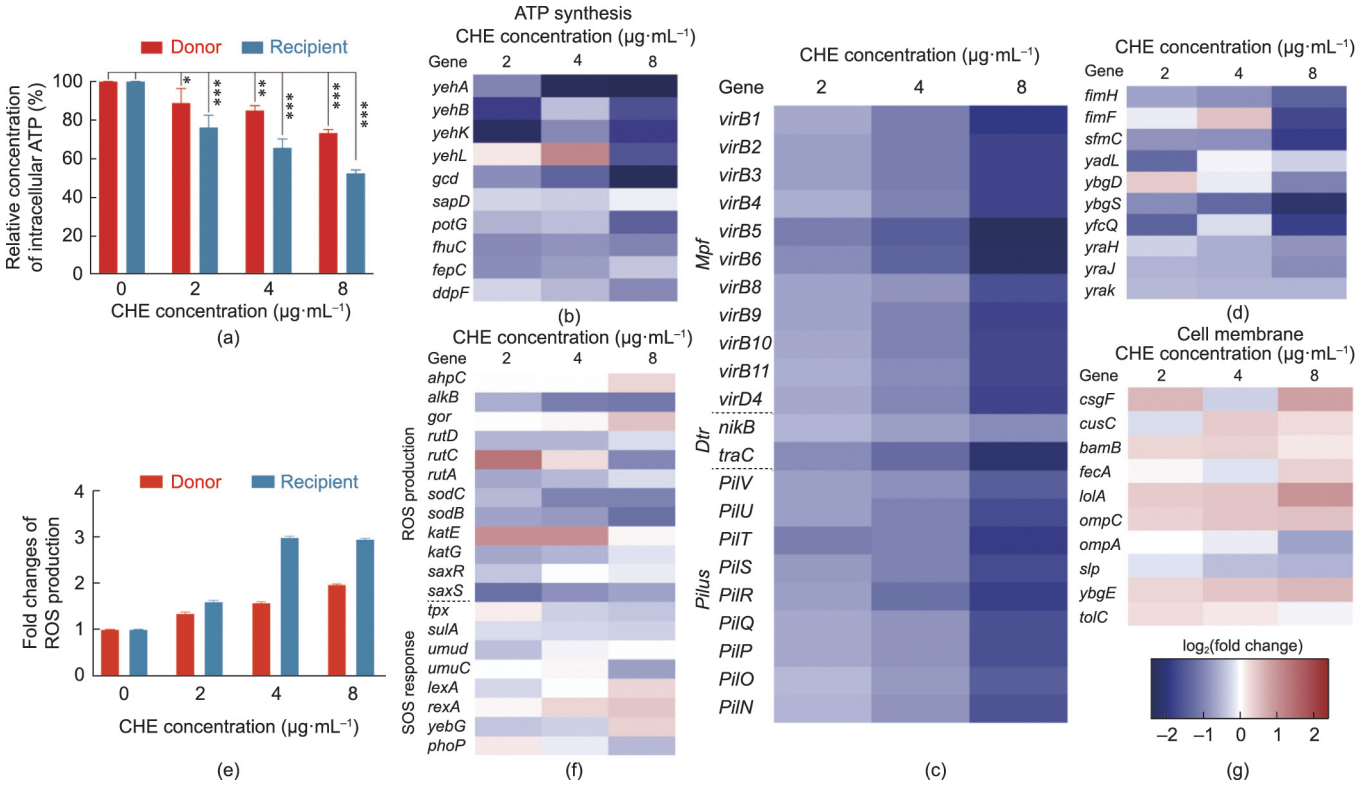

Fig. 5. Mechanism of inhibiting conjugative transfer by CHE. (a) Relative intracellular ATP levels in donor and recipient bacteria. (b) Fold change in the expression of core genes related to ATP synthesis in donor bacteria. (c) Fold change in the expression of core conjugative-associated genes in IncI2 plasmid. (d) Fold change in the expression of core genes related to adhesive-pilus generation in donor bacteria. (e) Fold change in ROS production in donor and recipient bacteria. (f) Fold change in the expression of core genes related to ROS production and SOS response in donor bacteria. (g) Fold change in the expression of core genes related to the cell membrane in donor bacteria. *P* value was detected using one-way ANOVA and corrected using the Dunnett method. $^{*}P < 0.05$, $^{**}P < 0.01$, $^{***}P < 0.001$, $^{****}P < 0.0001$.

downregulation of ATP-synthesis-related genes in both the donor and recipient bacteria (Fig. 5(b); Tables S1 and S2, and Fig. S3(a) in the Appendix A). As decreased energy sources can inhibit conjugation efficiency [34], CHE-associated ATP depletion may contribute to decreasing the conjugative transfer of *mcr-1*-carrying IncI2 plasmid. Moreover, the transcription levels of genes related to DNA transfer and replication (*nikB* and *traC*), mating-pair formation (*virB1–virB11*), and the IncI-type plasmid unique IV pilus (*pilV*) involved in conjugation were downregulated from 1.5 to 7.3 times in both the donors and recipients in the presence of 2–8 μg·mL^{-1} CHE (Fig. 5(c); Table S3 in the Appendix A). Also, adhesion-relevant operons were significantly downregulated in the donor bacteria (e.g., *fim*-like yielded a 2.2-fold decrease in *fimH*; Fig. 5(d); Table S4 in the Appendix A). These operons are involved in the critical step of direct cell-to-cell contact in plasmid DNA transfer [35]. These results suggested that CHE inhibits plasmid conjugation by suppressing the expression of both pili-formation genes and conjugative transfer-related regulation genes.

3.7. CHE did not affect SOS response or membrane permeability

The oxidative stress-induced SOS response and membrane permeability damage promote conjugation [35,36]. ROS production was dose-dependently increased in the donor and recipient strains by 1.3- to 4.2-fold at 2, 4, and 8 μg·mL^{-1} CHE (Fig. 5(e)). However, neither the ROS- nor the SOS-related genes were significantly changed in the donor (Fig. 5(f); Table S5 in the Appendix A) or recipient strains (Fig. S3(b) and Table S6 in the Appendix A). An explanation for this finding could be that the CHE-related ATP decrease (Fig. 5(a)) may reduce the energy for the transcriptional expression of genes involved in ROS detoxification and SOS response [34]. Furthermore, membrane permeability was unchanged under CHE exposure (Fig. S2(c)). Compared with those in the control group, the transcriptome results showed no significant changes in the expression levels of inner or outer membrane-related genes in the donor (Fig. 5(g); Table S7 in the Appendix A) or recipient bacteria (Fig. S3(c)) and Table S8 in the Appendix A). Thus, the inhibitory effect of CHE on plasmid conjugative transfer was unaffected by the expression of ROS- or SOS-related genes, cell membrane-related genes, or cell membrane permeability. Therefore, we concluded that CHE at low concentrations limited the energy for conjugation and diminished the conjugation-related and pilus-related gene expressions, independent of the SOS response and the cell membrane permeability damage.

4. Discussion

The global emergence and fast spread of *mcr-1* and its high colonization levels in human and animal guts pose increasing threats to public health [4]. In this work, we proposed a new concept for controlling *mcr-1*-positive strains by using the dual effects of plant-derived CHE both *in vitro* and *in vivo*. CHE works synergistically with colistin against *mcr-1*-positive *E. coli* and inhibits the transfer of *mcr-1*-bearing plasmids. In addition to its anti-inflammatory [37], antitumor [38,39], and antiviral [40] bioactivities, CHE impairs cellular respiration, disrupts PMF, and decreases ATP levels by increasing plasma membrane fluidity, thereby limiting the function of efflux pumps and downregulating *mcr-1* and the genes involved in conjugation bioprocesses (Fig. 6). This forms the basis of CHE's dual effects: It reverses the colistin-resistant phenotype of *mcr-1*-positive strains and inhibits the conjugation of *mcr-1*-bearing plasmids. The dual effects of CHE are important, because

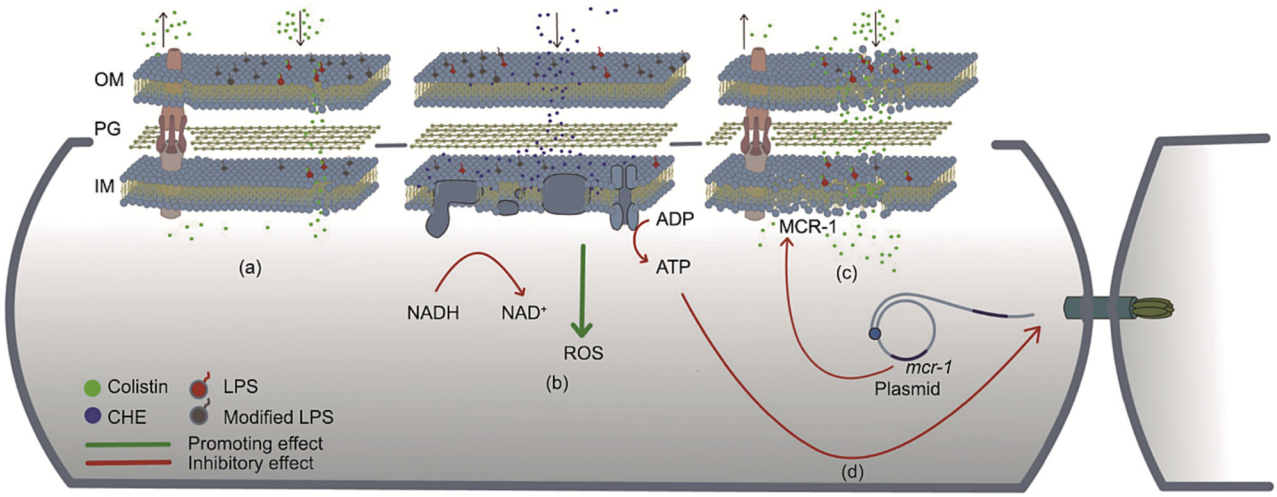

Fig. 6. Mechanisms of the dual effects of CHE in potentiating colistin efficacy and inhibiting the conjugative transfer of *mcr-1*-carrying IncI2 plasmids. (a) Without CHE, the LPS is modified by MCR-1, and colistin is expelled by efflux pumps, where it is difficult for colistin to disrupt the membrane structure. (b) CHE is able to penetrate into the phospholipid bilayers of the plasma membrane and increase the fluidity of the membrane, which inhibits the cellular respiration, disrupts the PMF, and generates ROS, leading to intracellular ATP depletion. (c) Since ATP is critically important, the function of *mcr-1* is limited and the ratio of modified lipid A declines; the function of the efflux pumps is also impaired, which reverses the colistin resistant phenotype. (d) The ATP level is decreased by CHE and the genes involved in the conjugation bioprocess are downregulated, leading to a lower conjugation rate. OM: outer membrane; IM: inner membrane.

they extend the lifespan of colistin as a critically important antimicrobial agent in both human and veterinary medicine, and may extend applications of colistin to eliminate *mcr-1*-positive bacteria in human and animal guts.

Commercially available CHE is one of the major active components extracted from *Macleaya cordata*—which was first recorded in *The Compendium of Materia Medica*, published in the 16th century—and has a long history of use in treating pertussis and chronic bronchitis [41]. In recent years, the restricted use of antimicrobial agents as growth promoters [2] has led to widespread use of *Macleaya cordata* extracts (Sangrovit) as feed additives in domestic livestock breeding to promote livestock growth in China, the United States, and Europe [42–44]. The amounts of Sangrovit in foreign markets have increased year by year since 2017 (up to 2.41 tons per year), including in the markets of north and south America, Europe, Japan, the Middle East, and Africa [45]. From 2017 to 2022, the cumulative sales of Sangrovit in China exceeded 400 tons, which is equivalent to over 20 million tons of compound feed. The extensive use of CHE for its dual effects in worldwide livestock systems may enhance the efficacy of colistin in veterinary medicine for treating intestinal infections caused by *mcr-1*-carrying pathogens. This increasing usage may also confer selective pressure on the gut bacteria that mediate CHE resistance and reverse conjugation blocking, which may eventually decrease the effectiveness of colistin as a veterinary medicine. Although CHE shows a more effective killing ability against cancer cells, high CHE doses may cause tissue-specific damage to normal cells [46,47], limiting its use for treating systemic infections. However, the low absorption and bioavailability of CHE via oral administration [48] imply that CHE may be a candidate for treating intestinal infections and eliminating XDR strains from the gut, as demonstrated herein. Notably, the estimated CHE dose (0.05 mg·kg^{-1}) that is commercially applied as an animal growth promoter is approximately 200 times lower than the dose we used to block *in vivo* conjugation (10 mg·kg^{-1}), indicating that additional *in vivo* investigations, such as structural modifications or appropriate dosage form designs, are needed in order for CHE to be used in humans and animals for the gut decolonization of *mcr* variant genes and their host bacteria.

The cell membrane is critical for bacterial survival and growth; therefore, it is a promising target for developing antimicrobial agents and adjuvants [20,49,50]. Membrane disruptors, such as colistin and SLAP-S25, function as both antimicrobial agents and adjuvants [15,49]. The ability to alter membrane fluidity is another key factor in antimicrobial activity [51–53]. Homeostasis of bacterial cytoplasmic membrane fluidity is vital to numerous cell functions, especially energy generation [54]. Here, we confirm that CHE interacts with PG and CL, thus rapidly and significantly increasing the cytoplasmic membrane fluidity and leading to physiological dysfunction in the bacteria, such as oxidative stress and energy depletion. As ATP plays vital roles in biosynthesis, metabolism regulation, and cellular maintenance [55,56], reducing intracellular ATP levels affects the bacterial resistant phenotype by limiting the expression of antimicrobial-resistance proteins such as MCR-1. Therefore, CHE may be more effective than MCR-1-specific inhibitors [21,57], because it extends the efficacy of colistin against all *mcr*-variant-carrying pathogens. Furthermore, reduced intracellular ATP levels limit the transcription of plasmid-conjugative genes and decrease the conjugation frequency, because this type of horizontal transfer of resistance genes is an energy-driven biological process. To date, some nonantibiotic pharmaceuticals, such as the nonsteroidal anti-inflammatory drug ibuprofen and the lipid-lowering drug gemfibrozil, have been shown to promote the horizontal gene transfer of XDR-carrying plasmids [58], while the discovery of conjugation inhibitors is rare and specific. For example, some unsaturated fatty acids can inhibit conjugation by binding to the plasmid-encoded T4SS component TraE [59]. While it is indispensable for bacterial energy metabolism, ATP has rarely been identified as a potential target for inhibiting conjugation. CHE can decrease bacterial ATP without increasing membrane permeability or significantly changing the expressions of SOS-response-related genes, the increase of which has been associated with promoting conjugation. For example, colistin has been shown to facilitate the transfer of antimicrobial resistance genes by increasing membrane permeability [7]. Our data indicate that increasing the bacterial plasma membrane fluidity to limit ATP generation but maintain membrane permeability is a promising strategy to combat antimicrobial resistance.

CHE has previously been shown to decrease intracellular ATP levels by inducing membrane damage [60]. However, we identified no obvious membrane destruction. These contradictory conclusions might be attributed to different time measures of the membrane status. We measured all physiological changes in the bacteria within 2 h of CHE treatment, when most cells were damaged but still survived. Conversely, Qian et al. [60] observed the bacteria 8 h after CHE treatment, which might have been too long to observe morphological or physiological changes that would show the primary antimicrobial mechanisms of CHE. In addition, we observed oxidative stress after 30 min of CHE treatment, suggesting that more time is needed for CHE to cause membrane damage [61]. Thus, we concluded that the antimicrobial mechanisms of CHE include targeting phospholipids, increasing membrane fluidity, and impairing bacterial respiration, followed by energy depletion and oxidative stress. Further studies are needed to fill the gaps in our understanding of the relationship between CHE's increasing membrane fluidity and decreasing bacterial respiratory rates.

5. Conclusions

Herein, we identified the dual effects of feed additive-derived CHE in enhancing colistin's ability to combat *mcr-1*-positive pathogens and inhibit the horizontal gene transfer of *mcr-1*-bearing plasmids by impairing energy generation and the conjugative transfer apparatus. Our results may provide guidance for determining additional antimicrobial-resistance-combating effects of known antimicrobial compounds and be a reference for future antimicrobial and adjuvant development.

Acknowledgments

This work was supported in part by grants from the Laboratory of Lingnan Modern Agriculture Project (NT2021006 to Yang Wang and Jianzhong Shen) and the National Natural Science Foundation of China (81861138051 and 81991535 to Yang Wang and Congming Wu).

Compliance with ethics guidelines

Huangwei Song, Xueyang Wang, Muchen Zhang, Zhiyu Zou, Siyuan Yang, Tian Yi, Jianfeng Wang, Dejun Liu, Yingbo Shen, Chongshan Dai, Zhihai Liu, Timothy R. Walsh, Jianzhong Shen, Congming Wu, and Yang Wang declare that they have no conflict of interest or financial conflicts to disclose.

Appendix A. Supplementary data

Supplementary data to this article can be found online at https://doi.org/10.1016/j.eng.2023.06.012.

References

[1] Li J, Nation RL, Turnidge JD, Milne RW, Coulthard K, Rayner CR, et al. Colistin: the re-emerging antibiotic for multidrug-resistant Gram-negative bacterial infections. Lancet Infect Dis 2006;6(9):589–601.
[2] Wang Y, Xu C, Zhang R, Chen Y, Shen Y, Hu F, et al. Changes in colistin resistance and *mcr-1* abundance in *Escherichia coli* of animal and human origins following the ban of colistin-positive additives in China: an epidemiological comparative study. Lancet Infect Dis 2020;20(10):1161–71.
[3] Liu Y, Wang Y, Walsh TR, Yi L, Zhang R, Spencer J, et al. Emergence of plasmid-mediated colistin resistance mechanism MCR-1 in animals and human beings in China: a microbiological and molecular biological study. Lancet Infect Dis 2016;16(2):161–8.
[4] Ling Z, Yin W, Shen Z, Wang Y, Shen J, Walsh TR. Epidemiology of mobile colistin resistance genes *mcr-1* to *mcr-9*. J Antimicrob Chemother 2020;75(11):3087–95.
[5] Andrade FF, Silva D, Rodrigues A, Pina-Vaz C. Colistin update on its mechanism of action and resistance, present and future challenges. Microorganisms 2020;8(11):1716.
[6] Sun J, Zhang H, Liu Y, Feng Y. Towards understanding MCR-like colistin resistance. Trends Microbiol 2018;26(9):794–808.
[7] Xiao X, Zeng F, Li R, Liu Y, Wang Z. Subinhibitory concentration of colistin promotes the conjugation frequencies of *mcr-1*- and bla_{NDM-5}-positive plasmids. Microbiol Spectr 2022;10(2):e02160-21.
[8] McEwen SA, Collignon PJ. Antimicrobial resistance: a one health perspective. Microbiol Spectr 2018;6(2):ARBA-0009-2017.
[9] Hernando-Amado S, Coque TM, Baquero F, Martínez JL. Defining and combating antibiotic resistance from one health and global health perspectives. Nat Microbiol 2019;4(9):1432–42.
[10] Wang Y, Tian GB, Zhang R, Shen Y, Tyrrell JM, Huang X, et al. Prevalence, risk factors, outcomes, and molecular epidemiology of *mcr-1*-positive Enterobacteriaceae in patients and healthy adults from China: an epidemiological and clinical study. Lancet Infect Dis 2017;17(4):390–9.
[11] Outterson K, Powers JH, Daniel GW, McClellan MB. Repairing the broken market for antibiotic innovation. Health Aff 2015;34(2):277–85.
[12] Payne DJ, Miller LF, Findlay D, Anderson J, Marks L. Time for a change: addressing R&D and commercialization challenges for antibacterials. Philos Trans R Soc Lond B Biol Sci 2015;370(1670):20140086.
[13] Wright GD. Opportunities for natural products in 21st century antibiotic discovery. Nat Prod Rep 2017;34(7):694–701.
[14] Tyers M, Wright GD. Drug combinations: a strategy to extend the life of antibiotics in the 21st century. Nat Rev Microbiol 2019;17(3):141–55.
[15] MacNair CR, Stokes JM, Carfrae LA, Fiebig-Comyn AA, Coombes BK, Mulvey MR, et al. Overcoming *mcr-1* mediated colistin resistance with colistin in combination with other antibiotics. Nat Commun 2018;9:458.
[16] Liu Y, Li R, Xiao X, Wang Z. Antibiotic adjuvants: an alternative approach to overcome multi-drug resistant Gram-negative bacteria. Crit Rev Microbiol 2019;45(3):301–14.
[17] Wright GD. Antibiotic adjuvants: rescuing antibiotics from resistance. Trends Microbiol 2016;24(11):862–71.
[18] Moloney MG. Natural products as a source for novel antibiotics. Trends Pharmacol Sci 2016;37(8):689–701.
[19] Genilloud O. Natural products discovery and potential for new antibiotics. Curr Opin Microbiol 2019;51:81–7.
[20] Song M, Liu Y, Li T, Liu X, Hao Z, Ding S, et al. Plant natural flavonoids against multidrug resistant pathogens. Adv Sci 2021;8(15):e2100749.
[21] Zhou Y, Liu S, Wang T, Li H, Tang S, Wang J, et al. Pterostilbene, a potential MCR-1 inhibitor that enhances the efficacy of polymyxin B. Antimicrob Agents Chemother 2018;62(4):e02146-17.
[22] Zhang R, Dong N, Huang Y, Zhou H, Xie M, Chan EWC, et al. Evolution of tigecycline- and colistin-resistant CRKP (carbapenem-resistant *Klebsiella pneumoniae*) *in vivo* and its persistence in the GI tract. Emerg Microbes Infect 2018;7:127.
[23] Saeloh D, Tipmanee V, Jim KK, Dekker MP, Bitter W, Voravuthikunchai SP, et al. The novel antibiotic rhodomyrtone traps membrane proteins in vesicles with increased fluidity. PLoS Pathog 2018;14(2):e1006876.
[24] Sabnis A, Hagart KL, Klöckner A, Becce M, Evans LE, Furniss RCD, et al. Colistin kills bacteria by targeting lipopolysaccharide in the cytoplasmic membrane. eLife 2021;10:e65836.
[25] Altman FP. Tetrazolium salts and formazans. Prog Histochem Cytochem 1976;9(3):1–51.
[26] Ansó E, Weinberg SE, Diebold LP, Thompson BJ, Malinge S, Schumacker PT, et al. The mitochondrial respiratory chain is essential for haematopoietic stem cell function. Nat Cell Biol 2017;19(6):614–25.
[27] Meylan S, Porter CBM, Yang JH, Belenky P, Gutierrez A, Lobritz MA, et al. Carbon sources tune antibiotic susceptibility in *Pseudomonas aeruginosa* via tricarboxylic acid cycle control. Cell Chem Biol 2017;24(2):195–206.
[28] Orazi G, Ruoff KL, O'Toole GA. *Pseudomonas aeruginosa* increases the sensitivity of biofilm-grown *Staphylococcus aureus* to membrane-targeting antiseptics and antibiotics. MBio 2019;10(4):e01501–e1519.
[29] Parasassi T, Gratton E. Membrane lipid domains and dynamics as detected by Laurdan fluorescence. J Fluoresc 1995;5(1):59–69.
[30] Fang G, Li W, Shen X, Perez-Aguilar JM, Chong Y, Gao X, et al. Differential Pd-nanocrystal facets demonstrate distinct antibacterial activity against Gram-positive and Gram-negative bacteria. Nat Commun 2018;9:129.
[31] Baron SA, Rolain JM. Efflux pump inhibitor CCCP to rescue colistin susceptibility in *mcr-1* plasmid-mediated colistin-resistant strains and Gram-negative bacteria. J Antimicrob Chemother 2018;73(7):1862–71.
[32] Cheng YH, Lin TL, Lin YT, Wang JT. A putative RND-type efflux pump, H239_3064, contributes to colistin resistance through CrrB in *Klebsiella pneumoniae*. J Antimicrob Chemother 2018;73(6):1509–16.
[33] Cabezón E, Ripoll-Rozada J, Peña A, de la Cruz F, Arechaga I. Towards an integrated model of bacterial conjugation. FEMS Microbiol Rev 2015;39(1):81–95.
[34] Huang H, Liao J, Zheng X, Chen Y, Ren H. Low-level free nitrous acid efficiently inhibits the conjugative transfer of antibiotic resistance by altering intracellular ions and disabling transfer apparatus. Water Res 2019;158:383–91.
[35] Wang Y, Lu J, Mao L, Li J, Yuan Z, Bond PL, et al. Antiepileptic drug carbamazepine promotes horizontal transfer of plasmid-borne multi-

antibiotic resistance genes within and across bacterial genera. ISME J 2019;13(2):509–22.
[36] Beaber JW, Hochhut B, Waldor MK. SOS response promotes horizontal dissemination of antibiotic resistance genes. Nature 2004;427(6969):72–4.
[37] Pěnčíková K, Kollár P, Závalová VM, Táborská E, Urbanová J, Hošek J. Investigation of sanguinarine and chelerythrine effects on LPS-induced inflammatory gene expression in THP-1 cell line. Phytomedicine 2012;19(10):890–5.
[38] Chmura SJ, Dolan ME, Cha A, Mauceri HJ, Kufe DW, Weichselbaum RR. *In vitro* and *in vivo* activity of protein kinase C inhibitor chelerythrine chloride induces tumor cell toxicity and growth delay *in vivo*. Clin Cancer Res 2000;6(2):737–42.
[39] Platzbecker U, Ward JL, Deeg HJ. Chelerythrin activates caspase-8, downregulates FLIP long and short, and overcomes resistance to tumour necrosis factor-related apoptosis-inducing ligand in KG1a cells. Br J Haematol 2003;122(3):489–97.
[40] Valipour M, Zarghi A, Ebrahimzadeh MA, Irannejad H. Therapeutic potential of chelerythrine as a multi-purpose adjuvant for the treatment of COVID-19. Cell Cycle 2021;20(22):2321–36.
[41] Huang X, Yang M, Lei J. Research of celandine in the treatment of cough and asthma. Jilin J Chin Med 2017;37(7):725–76.
[42] Li B, Zhang JQ, Han XG, Wang ZL, Xu YY, Miao JF. Macleaya cordata helps improve the growth-promoting effect of chlortetracycline on broiler chickens. J Zhejiang Univ Sci B 2018;19(10):776–84.
[43] Huang CY, Huang YJ, Zhang ZY, Liu YS, Liu ZY. Metabolism and tissue distribution of chelerythrine and effects of Macleaya cordata extracts on liver NAD(P)H quinone oxidoreductase. Front Vet Sci 2021;8:659771.
[44] Wang W, Dolan LC, von Alvensleben S, Morlacchini M, Fusconi G. Safety of standardized *Macleaya cordata* extract in an eighty-four-day dietary study in dairy cows. J Anim Physiol Anim Nutr 2018;102(1):e61–8.
[45] QYResearch. 2023−2029 Global and China *Macleaya cordata* extract industry research and 14th Five Year Plan analysis report. Report. Beijing: QYResearch; 2022.
[46] Gao L, Schmitz HJ, Merz KH, Schrenk D. Characterization of the cytotoxicity of selected *Chelidonium alkaloids* in rat hepatocytes. Toxicol Lett 2019;311:91–7.
[47] Wang J, Song Y, Zhang N, Li N, Liu C, Wang B. Using liposomes to alleviate the toxicity of chelerythrine, a natural pkc inhibitor, in treating non-small cell lung cancer. Front Oncol 2021;11:658543.
[48] Hu N, Chen M, Liu Y, Shi Q, Yang B, Zhang H, et al. Pharmacokinetics of sanguinarine, chelerythrine, and their metabolites in broiler chickens following oral and intravenous administration. J Vet Pharmacol Ther 2019;42(2):197–206.
[49] Song M, Liu Y, Huang X, Ding S, Wang Y, Shen J, et al. A broad-spectrum antibiotic adjuvant reverses multidrug-resistant Gram-negative pathogens. Nat Microbiol 2020;5(8):1040–50.
[50] Yeaman MR, Yount NY. Mechanisms of antimicrobial peptide action and resistance. Pharmacol Rev 2003;55(1):27–55.
[51] Müller A, Wenzel M, Strahl H, Grein F, Saaki TNV, Kohl B, et al. Daptomycin inhibits cell envelope synthesis by interfering with fluid membrane microdomains. Proc Natl Acad Sci USA 2016;113(45):E7077–86.
[52] Kim W, Zou G, Hari TPA, Wilt IK, Zhu W, Galle N, et al. A selective membrane-targeting repurposed antibiotic with activity against persistent methicillin-resistant *Staphylococcus aureus*. Proc Natl Acad Sci USA 2019;116(33):16529–34.
[53] Dombach JL, Quintana JLJ, Detweiler CS. Staphylococcal bacterial persister cells, biofilms, and intracellular infection are disrupted by JD1, a membrane-damaging small molecule. MBio 2021;12(5):e01801–21.
[54] Mykytczuk NCS, Trevors JT, Leduc LG, Ferroni GD. Fluorescence polarization in studies of bacterial cytoplasmic membrane fluidity under environmental stress. Prog Biophys Mol Biol 2007;95(1–3):60–82.
[55] Löffler M, Simen JD, Jäger G, Schäferhoff K, Freund A, Takors R. Engineering *E. coli* for large-scale production—strategies considering ATP expenses and transcriptional responses. Metab Eng 2016;38:73–85.
[56] Yu T, Zhou YJ, Huang M, Liu Q, Pereira R, David F, et al. Reprogramming yeast metabolism from alcoholic fermentation to lipogenesis. Cell 2018;174(6):1549–1558.e14.
[57] Guo Y, Lv X, Wang Y, Zhou Y, Lu N, Deng X, et al. Honokiol restores polymyxin susceptibility to MCR-1-positive pathogens both *in vitro* and *in vivo*. Appl Environ Microbiol 2020;86(5):e02346-19.
[58] Wang Y, Lu J, Zhang S, Li J, Mao L, Yuan Z, et al. Non-antibiotic pharmaceuticals promote the transmission of multidrug resistance plasmids through intra- and intergenera conjugation. ISME J 2021;15(9):2493–508.
[59] Getino M, Sanabria-Ríos DJ, Fernández-López R, Campos-Gómez J, Sánchez-López JM, Fernández A, et al. Synthetic fatty acids prevent plasmid-mediated horizontal gene transfer. MBio 2015;6(5):e01032–e15.
[60] Qian WD, Huang J, Zhang JN, Li XC, Kong Y, Wang T, et al. Antimicrobial and antibiofilm activities and mechanism of action of chelerythrine against carbapenem-resistant *Serratia marcescens in vitro*. Microb Drug Resist 2021;27(8):1105–16.
[61] Kajarabille N, Latunde-Dada GO. Programmed cell-death by ferroptosis: antioxidants as mitigators. Int J Mol Sci 2019;20(19):4968.